Identification of Isomeric *meso*-Dioxo Derivatives of Octaethylporphyrin and Separation and Structural Characterization of the Nickel(II) Complexes

Alan L. Balch,* Marilyn M. Olmstead, and Shane L. Phillips

Department of Chemistry, University of California, Davis, California 95616

Received March 17, 1993

Oxidation of Zn^{II}(OEP) (OEP is the dianion of octaethylporphyrin) with thallium(III) trifluoroacetate is shown to form the previously unknown *cis*-dioxooctaethylporphodimethene (*cis*-H_2OEPO_2) as well as the known, isomeric *trans*-dioxooctaethylporphodimethene (*trans*-H_2OEPO_2). While these have not been separated, their nickel (II) complexes are readily separated by chromatography on silica gel. Electronic absorption and ^1H NMR spectra are reported for these diamagnetic planar complexes. Addition of pyridine to either Ni(*trans*-$OEPO_2$) or Ni(*cis*-$OEPO_2$) yields six-coordinate, paramagnetic ($S = 1$) adducts. Dark violet Ni^{II}(*cis*-$OEPO_2$), $C_{36}H_{42}N_4NiO_2$, crystallizes in the tetragonal space group $I4_1/a$ with $a = 14.664(7)$ Å and $c = 14.163(7)$ Å at 130 K with $Z = 4$. Refinement of 745 reflections and 102 parameters yields $R = 0.039$, $R_w = 0.043$. The nickel is four-coordinate (Ni–N distance is 1.912(3) Å), and its coordination geometry is planar, while the macrocycle displays a saddle-shaped distortion. The keto groups are disordered over the four meso positions. Crystallization of Ni^{II}(*trans*-$OEPO_2$) from pyridine yields dark orange $(py)_2$Ni(*trans*-$OEPO_2$), $C_{46}H_{50}N_6NiO_2$, which crystallizes in the triclinic space group $P\bar{1}$ with $a = 9.878(4)$ Å, $b = 10.212(4)$ Å, $c = 10.503(4)$ Å, $\alpha = 80.08(3)°$, $\beta = 89.28(3)°$, and $\gamma = 66.50(3)°$ at 130 K with $Z = 1$. Refinement of 2149 reflections and 260 parameters yields $R = 0.030$, $R_w = 0.040$. The structure consists of a six-coordinate nickel ion at the center of the nearly planar macrocycle with the oxygen atoms disordered unequally into two sites so that it is clear that the *trans*-dioxo unit is present.

Introduction

The oxidation of octaethylporphyrin (H_2OEP) and its metal complexes by thallium(III) trifluoroacetate yields a variety of meso-oxygenated products.[1-4] These include the oxophlorins **1**, the α,γ-dioxoporphodimethene **2**, the α,β,γ-trioxo compound **3**, and the xanthoporphyrinogen **4**. As part of studies in this laboratory of the oxidation products formed in the reaction of iron porphyrins with dioxygen,[5-7] it became important to learn whether this oxidation ever proceeded further than the formation of the iron oxophlorin complexes to form di- and possibly tri- and tetraoxo species. Air oxidation of iron porphyrins in the presence of a reducing agent (coupled oxidation)[8-10] has been widely used as a model for the catabolism of heme by heme oxygenase.[11-13] This enzyme initiates the oxidation of heme that eventually results in the formation of bilirubin, the yellow pigment that causes jaundice.

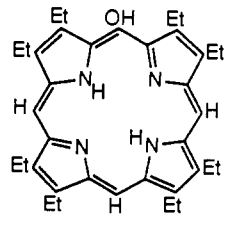

1 (H_2OEPOH)

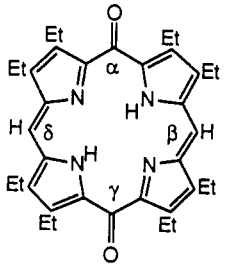

2(*trans*-H_2OEPO_2)

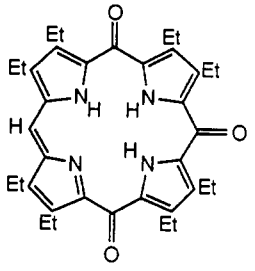

3

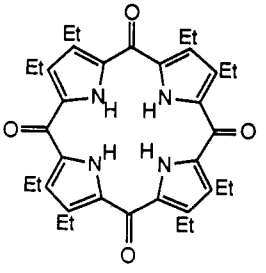

4

In order to be able to identify the dioxoporphodimethene, **2**, and its iron complexes, we initially re-examined the products of the oxidation of Zn^{II}(OEP) by thallium(III) trifluoroacetate. In examining the insertion of nickel(II) into **2**, we found that the material previously described as **2** was really a mixture of the *trans* complex **2** along with a significant amount (20%) of the *cis* isomer, **5**. Here we report on the separation of the nickel(II) complexes of **2** and **5** and describe spectroscopic and structural studies on these complexes.

Results

Separation and Spectroscopic Characterization of the Nickel(II) Complexes. The oxidation of Zn^{II}(OEP) with thallium (III) trifluoroacetate was conducted as described earlier, and the orange-brown fraction that was previously identified as the *trans*-dioxoporphodimethene, **2**, was collected after chromatography on alumina. The 300 MHz ^1H NMR spectrum of this fraction

(1) Barnett, G. H.; Hudson, M. F.; McCombie, S. W.; Smith, K. M. *J. Chem. Soc., Perkin Trans.* **1973**, 691.
(2) Barnett, G. H.; Evans, B.; Smith, K. M. *Tetrahedron* **1975**, *31*, 2711.
(3) Fuhrhop, J.-H.; Besecke, S.; Subramanian, J.; Mengersen, Chr.; Riesner, D. *J. Am. Chem. Soc.* **1975**, *97*, 7141.
(4) Fuhrhop, J.-H.; Baumgartner, E.; Baur, H. *J. Am. Chem. Soc.* **1981**, *103*, 5854.
(5) Balch, A. L.; Latos-Grażyński, L.; Noll, B. C.; Olmstead, M. M.; Zovinka, E. P. *Inorg. Chem.* **1992**, *31*, 2248.
(6) Balch, A. L.; Latos-Grażyński, L.; Noll, B. C.; Olmstead, M. M.; Szterenberg, L.; Safari, N. *J. Am. Chem. Soc.* **1993**, *115*, 1422.
(7) Balch, A. L.; Latos-Grażyński, L.; Noll, B. C.; Olmstead, M. M.; Safari, N., submitted for publication.
(8) Lemberg, R. *Rev. Pure Appl. Chem.* **1956**, *6*, 1.
(9) Bonnett, R.; Dimsdale, M. J. *J. Chem. Soc., Perkin Trans 1* **1972**, 2540.
(10) Lagarias, J. C. *Biochim. Biophys. Acta* **1982**, *717*, 12.
(11) O'Cara, P. In *Porphyrins and Metalloporphyrins*; Smith, K. M., Ed.; Elsevier: New York, 1975; p 123.
(12) Schmid, R.; McDonagh, A. F. In *The Porphyrins*; Dolphin, D. Ed.; Academic Press: New York, 1979; Vol. 6, p 258.
(13) Bissell, D. M. In *Liver: Normal Function and Disease*; Ostrow, J. D., Ed.; Marcel Decker, Inc.: New York, 1986; Vol. 4, p 133.

0020-1669/93/1332-3931$04.00/0

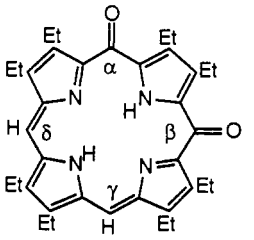

5 (*cis*-H_2OEPO_2)

clearly showed that it consisted primarily of the *trans*-dioxo compound, **2**, with spectral properties in agreement with those reported earlier.[2] However, a minor component, which represents about 20% of the sample, was also apparent. Relevant ^1H NMR spectral data are shown in Figure 1. The meso region in part III shows a distinct feature that is upfield of the singlet of **2**, and the region of the N–H resonances shown in part IV reveals two equally intense features that are also upfield of the singlet from **2**. The methyl and methylene regions shown in parts I and II of the figure also show some weak features that are indicative of the presence of the second component. The observation of two N–H resonances and one meso resonance is consistent with the presence of the *cis*-dioxo compound **5** but alone certainly does not conclusively establish its identity. Further attempts to separate the entity responsible for these additional features were not successful. However, after metalation with nickel(II), a separation of the two isomers as the nickel(II) complexes was achieved.

The metalation was accomplished by treatment of the mixture of the macrocycles with nickel(II) acetate in boiling acetic acid. The green solution became orange as metalation proceeded. The product of metalation was subjected to chromatography on silica gel, which allowed the separation of a faster eluting band of ochre Ni^{II}(*trans*-$OEPO_2$) (**6**) from the violet band of Ni^{II}(*cis*-$OEPO_2$) (**7**). Evaporation yielded the complexes in crystalline form. Electron impact mass spectra of the two individual isomers show intense parent ion peaks for each at m/z = 620 amu with isotopic cluster abundances that agree with the calculated pattern.

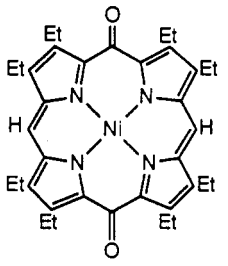

6 (Ni^{II}(*trans*-$OEPO_2$))

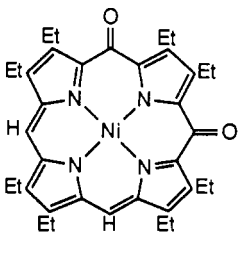

7 (Ni^{II}(*cis*-$OEPO_2$))

The ^1H NMR spectra of **6** and **7** in chloroform solutions are compared to one another and to that of the free-ligand mixture in Figure 1. The observation of well-resolved spectra in the 0–10 ppm region indicates that these complexes are diamagnetic and therefore that the nickel has planar, four-coordinate geometry. The patterns of resonances for **6** and **7** are in accord with their idealized symmetry: D_{2h} for **6**, C_{2v} for **7**. Each shows only a single meso resonance; that of **7** is upfield of that of **6** as seen in part III of Figure 1. For **6** there are two overlapping methyl triplets and two methylene quartets. In accord with its lower symmetry, **7** has a more complex spectrum with four, equally intense methylene quartets and four methyl triplets.

The infrared spectra of these isomers as mineral oil mulls show clear evidence for the presence of the keto substituents. For **6**, the C–O stretch appears as a strong band at 1600 cm^{-1} with a shoulder at 1627 cm^{-1}, while for **7** two bands are observed at 1732 and 1589 cm^{-1}.

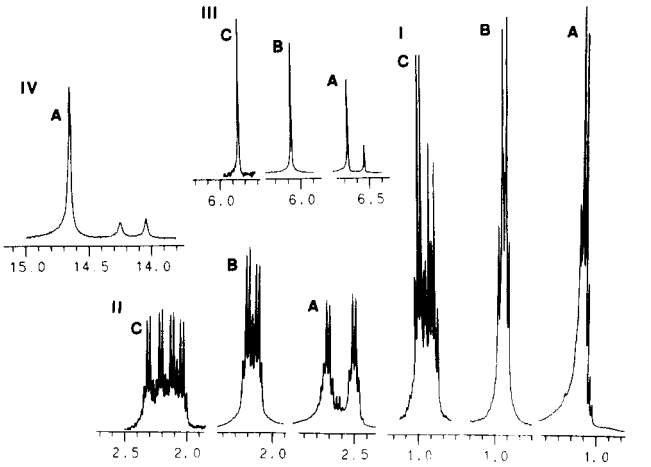

Figure 1. 300-MHz ^1H NMR spectra of chloroform solutions of (A) a mixture of **2** and **5** after chromatographic purification, (B) Ni^{II}(*trans*-$OEPO_2$), and (C) Ni^{II}(*cis*-$OEPO_2$): I, methyl region; II, methylene region; III, meso region; IV, NH region. The relative intensities in regions I–III are plotted to the same scale for each compound. The intensity for region IV for (A) is enhanced 5-fold relative to regions I–III.

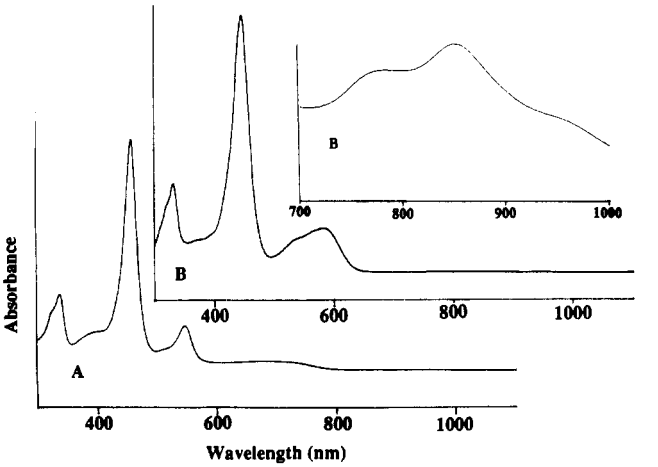

Figure 2. Electronic absorption spectra of Ni^{II}(*trans*-$OEPO_2$) in (A) dichloromethane and (B) pyridine at 23 °C.

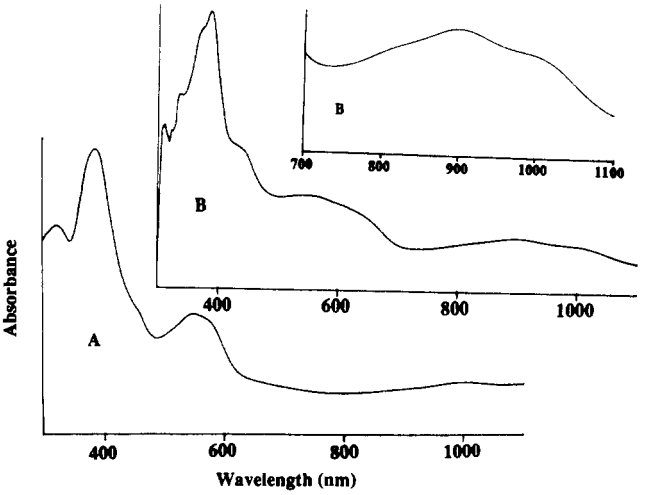

Figure 3. Electronic absorption spectra of Ni^{II}(*cis*-$OEPO_2$) in (A) dichloromethane and (B) pyridine solution at 23 °C.

The electronic absorption spectra of **6** and **7** are given in Figures 2 and 3, respectively. In chloroform solution both show porphyrin-like spectra, but that of the *cis* isomer, **7**, is markedly broader and less intense and shows unusual low-energy absorptions at 897 nm (a shoulder) and at 991 nm. Dissolution of the complexes in

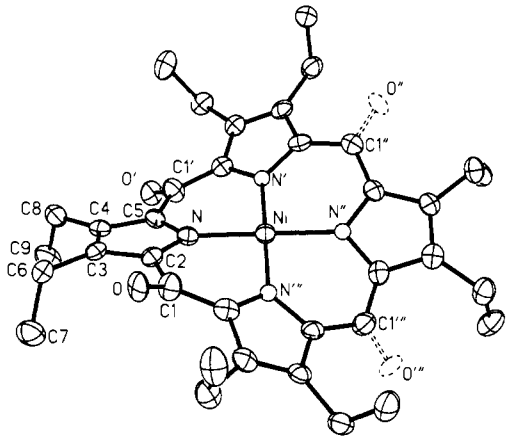

Figure 4. Perspective view of Ni^{II}(*cis*-$OEPO_2$) with 50% thermal contours for all atoms. Each of the four oxygen atom sites has only half-occupancy.

pyridine produces noticeable spectral shifts, as seen in these two figures. These shifts suggest that pyridine is coordinated to the nickel ion.

The formation of pyridine adducts, $(py)_2Ni^{II}$(*trans*-$OEPO_2$) and $(py)_2Ni^{II}$(*cis*-$OEPO_2$), has been confirmed by ^1H NMR spectral studies and by isolation of the adducts in crystalline form. The sharp ^1H NMR resonances of **6** and **7** that are observed in chloroform are no longer present in pyridine solution. They are replaced by broader resonances that are indicative of the formation of paramagnetic adducts. For **6** in pyridine-d_5 at 22 °C, three broad resonances at 10.2, 1.7, and −8.2 ppm are assigned to the methylene, methyl, and meso groups, respectively, on the basis of their relative integrated intensities. Additionally, the shift pattern, with the absolute magnitude of the hyperfine shifts in the order meso > methylene > methyl, follows that generally seen for paramagnetic complexes of octaethylporphyrin and its derivatives.[5,6] The line widths for these resonances (80 Hz (methylene), 60 Hz (methyl), and 350 Hz (meso)) are consistent with the paramagnetic character of the pyridine adduct. Because of the broad lines observed for this adduct, the two individual methyl and methylene resonances are not resolved. For **7** in pyridine-d_5 at 22 °C, a similar, but distinct, set of resonances at 11.1, 1.77, and −10.7 ppm with line widths of 80, 80, and 350 Hz are observed and assigned to the methylene, methyl, and meso groups, respectively. As with **6**, the lines are broad and the individual methylene and methyl resonances have not been resolved.

In pyridine-d_5 solution at 23 °C, the magnetic moment of $(py)_2Ni^{II}$(*trans*-$OEPO_2$) is 2.6(3) μ_B. This is consistent with the presence of six-coordinate nickel(II) with an $S = 1$ spin state.

Crystal and Molecular Structures of Ni^{II}(*cis*-$OEPO_2$) (7) and Ni^{II}(*trans*-$OEPO_2$) (6). The structures of crystalline samples of both isomers have been examined by X-ray crystallography. Ni^{II}(*cis*-$OEPO_2$) (**7**) crystallizes in the tetragonal space group $I4_1/a$ and is isomorphous with the tetragonal modification of Ni^{II}(OEP)[14] and with disordered Ni^{II}(OEPOH).[15] The complex has crystallographically imposed S_4 symmetry, and the asymmetic unit consists of one-quarter of a nickel atom, one pyrrole ring with two ethyl groups, and one meso carbon with its substituent (one-half of a hydrogen and oxygen atom). Thus, the structure is disordered, and the relative orientations of the two oxo substituents cannot be ascertained. A view of the molecule is shown in Figure 4. Atomic coordinates are presented in Table I. Table II contains selected interatomic distances and angles.

The nickel ion is planar and four-coordinate. The Ni–N distance (1.912(3) Å) is similar to the analogous distances in Ni^{II}(OEP) (1.929(3) Å[14] and Ni^{II}(OEPOH) (1.921(6) Å).[15]

Table I. Atomic Coordinates (×10^4) and Equivalent Isotropic Displacement Coefficients (Å^2 × 10^3) for Ni^{II}(*cis*-$OEPO_2$)[a]

	x	*y*	*z*	*U*(eq)[b]
Ni	0	7500	3750	25(1)
N	49(2)	6197(2)	3743(2)	25(1)
O	2066(3)	5541(3)	4877(4)	35(2)
C(1)	1619(3)	5985(3)	4302(3)	36(1)
C(2)	759(2)	5645(2)	4026(2)	27(1)
C(3)	538(2)	4702(2)	3912(2)	27(1)
C(4)	−314(2)	4680(2)	3520(2)	30(1)
C(5)	−615(2)	5604(2)	3438(2)	28(1)
C(6)	1160(3)	3904(2)	4124(3)	35(1)
C(7)	1818(3)	3694(3)	3336(3)	48(2)
C(8)	−859(3)	3848(3)	3244(3)	38(1)
C(9)	−737(3)	3611(3)	2211(3)	46(2)

[a] O(1) was refined at 0.5 of normal occupancy. [b] Equivalent isotropic *U* defined as one-third of the trace of the orthogonalized U_{ij} tensor.

Table II. Bond Lengths and Angles for Ni^{II}(*cis*-$OEPO_2$)[a]

Bond Lengths (Å)			
Ni–N	1.912(3)	N–C(2)	1.379(4)
N–C(5)	1.375(4)	O–C(1)	1.223(6)
C(1)–C(2)	1.411(5)	C(2)–C(3)	1.429(5)
C(3)–C(4)	1.368(5)	C(4)–C(5)	1.429(5)
C(5)–C(1′)	1.422(5)		
Bond Angles (deg)			
N–Ni–N″	179.4(2)	N–Ni–N′	90.0(1)
Ni–N–C(2)	127.9(2)	Ni–N–C(5)	127.4(2)
C(2)–N–C(5)	104.7(3)	O–C(1)–C(2)	118.2(4)
O–C(1)–C(5‴)	119.9(4)	C(2)–C(1)–C(5‴)	121.2(3)
N–C(2)–C(1)	123.2(3)	N–C(2)–C(3)	111.4(3)
C(1)–C(2)–C(3)	125.2(3)	C(2)–C(3)–C(4)	106.0(3)
C(3)–C(4)–C(5)	107.0(3)	N–C(5)–C(4)	110.8(3)
N–C(5)–C(1′)	123.5(3)	C(4)–C(5)–C(1′)	125.2(3)

[a] Symmetry codes: ′ = −0.75+*y*, 0.75−*x*, 0.75−*z*; ‴ = 0.75−*y*, 0.75+x, 0.75−*z*.

The macrocycle is severely distorted into a saddle shape that is also observed in Ni^{II}(OEP) and Ni^{II}(OEPOH). This is readily seen in Figure 5A, which shows a diagram of the core with the out-of-plane distances for each atom. The C–O distance (1.223(6) Å) is consistent with the presence of a keto substituent.

Ni^{II}(*trans*-$OEPO_2$) has also been obtained in crystalline form and examined by X-ray diffraction. As reported in the Experimental Section, the crystals are isomorphous with those of the *cis* isomer. Thus, it too assumes a saddle-shaped geometry in the solid state.

Crystal and Molecular Structure of $(py)_2Ni^{II}$(*trans*-$OEPO_2$). Crystals of the complex that were suitable for X-ray diffraction were obtained by diffusion of methanol into a pyridine solution of **6**. These are isomorphous with those of $(py)_2Ni$(OEPO•) ((OEP)O• is the dianion π-radical obtained by deprotonation and one-electron oxidation of H_2OEPOH).[15] A view of the structure of $(py)_2Ni^{II}$(*trans*-$OEPO_2$) is given in Figure 6. Atomic coordinates are listed in Table III. Table IV contains a selected group of interatomic distances and angles.

The nickel ion, which sits at a center of symmetry, has six-coordinate geometry with bonds to the four pyrrole nitrogens and to the two axial pyridine ligands. The in-plane Ni–N(pyrrole) distances (2.067(2) and 2.074(2) Å) are longer than the Ni–N distance (1.912(3) Å) in four-coordinate Ni^{II}(*cis*-$OEPO_2$) or the Ni–N distance in the tetragonal form of four-coordinate Ni^{II}(OEP) (1.929(3) Å).[14] However, they are similar to the Ni–N distances (2.024(4) and 2.052(4) Å) seen in six-coordinate, paramagnetic ($S = 1$) $[(Im)_2Ni^{II}(TMPyP)](ClO_4)_4$.[16] The axial Ni–N(py) distance (2.223(2) Å) is even longer than the in-plane distances but is comparable to the corresponding Ni–N(Im)

(14) Meyer, E. F., Jr. *Acta Crystallogr.* **1972**, *B28*, 2162.
(15) Balch, A. L.; Noll, B. C.; Zovinka, E. P. Submitted for publication.
(16) Balch, A. L.; Noll, B. C.; Zovinka, E. P. *J. Am. Chem. Soc.* **1992**, *114*, 3380.

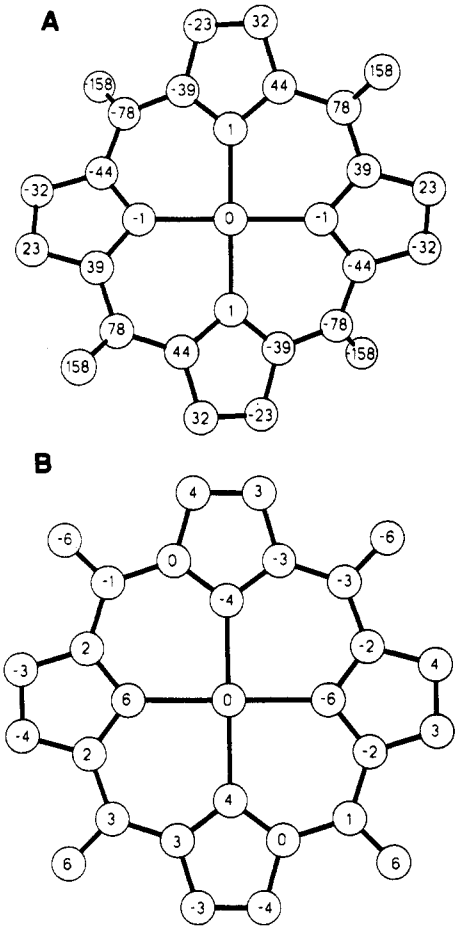

Figure 5. Diagrams of the cores of (A) Ni^{II}(*cis*-$OEPO_2$) and (B) $(py)_2Ni^{II}$(*trans*-$OEPO_2$). Each number represents the perpendicular displacement (in units of 0.01 Å) of that atom from the mean plane of the macrocycle.

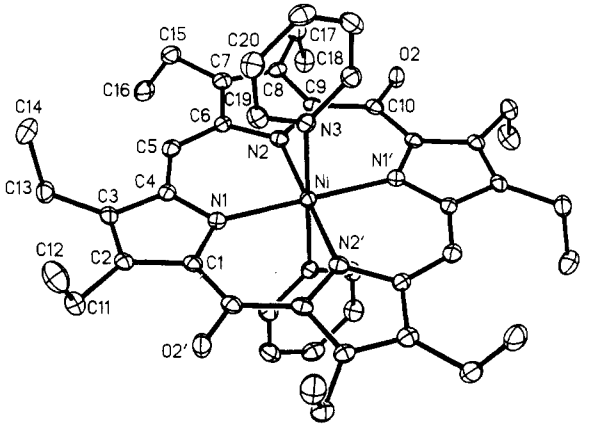

Figure 6. Perspective view of $(py)_2Ni^{II}$(*trans*-$OEPO_2$) with 50% thermal contours. The position of the major sites for the oxygen atoms (fractional occupancy 0.633) are shown. The minor sites are connected to C(5) and C(5′).

distance (2.160(4) Å) in $[(Im)_2Ni^{II}(TMPyP)](ClO_4)_4$.[16] Because of the site symmetry, the two pyridine ligands lie in the same plane. That plane makes an angle of 14.0° with the N(1)–Ni–N(1′) axis, an angle of 75.1° with the N(2)–Ni–N(2′) axis, and an angle of 2.2° with the NiN_4 plane. The core of the macrocyclic ligand in $(py)_2Ni^{II}$(*trans*-$OEPO_2$) is nearly planar. The out-of-plane atomic displacements shown in Figure 5B indicate that this six-coordinate complex lacks the severe saddle-shaped geometry seen in four-coordinate complexes like Ni^{II}(*cis*-$OEPO_2$).

Table III. Atomic Coordinates (×10⁴) and Equivalent Isotropic Displacement Coefficients (Å² × 10³) for $(py)_2Ni^{II}$(*trans*-$OEPO_2$)[a]

	x	*y*	*z*	*U*(eq)[b]
Ni	5000	5000	5000	14(1)
O(1)	6565(5)	748(5)	3194(4)	26(2)
O(2)	1385(3)	7493(2)	1500(2)	21(1)
N(1)	6647(2)	2936(2)	5498(2)	16(1)
N(2)	4366(2)	4463(2)	3356(2)	16(1)
N(3)	3446(2)	4222(2)	6104(2)	16(1)
C(1)	7615(2)	2366(2)	6570(2)	14(1)
C(2)	8505(2)	850(2)	6620(2)	15(1)
C(3)	8050(2)	487(2)	5544(2)	15(1)
C(4)	6904(2)	1800(2)	4861(2)	14(1)
C(5)	6126(2)	1899(2)	3694(2)	17(1)
C(6)	4947(2)	3126(2)	3004(2)	14(1)
C(7)	4163(2)	3130(2)	1852(2)	17(1)
C(8)	3094(2)	4503(2)	1500(2)	16(1)
C(9)	3239(2)	5315(2)	2456(2)	16(1)
C(10)	2321(2)	6824(2)	2452(2)	16(1)
C(11)	9704(2)	−160(2)	7626(2)	21(1)
C(12)	9130(3)	−838(3)	8795(2)	31(1)
C(13)	8544(2)	−991(2)	5201(2)	21(1)
C(14)	7499(3)	−1722(2)	5660(2)	26(1)
C(15)	4455(3)	1858(2)	1196(2)	23(1)
C(16)	5754(3)	1543(3)	323(2)	26(1)
C(17)	2014(2)	5052(2)	340(2)	22(1)
C(18)	2567(3)	5743(3)	−838(2)	27(1)
C(19)	3919(2)	2942(2)	6929(2)	19(1)
C(20)	2995(3)	2419(2)	7605(2)	23(1)
C(21)	1482(3)	3227(2)	7454(2)	23(1)
C(22)	975(3)	4538(3)	6618(2)	25(1)
C(23)	1976(2)	4998(2)	5969(2)	20(1)

[a] O(1) and O(2) represent a disordered pair with refined occupancies of 0.367(4) and 0.633(4), respectively. [b] Equivalent isotropic *U* defined as one-third of the trace of the orthogonalized U_{ij} tensor.

The positions of the meso oxo groups are disordered. The major sites with 0.633(4) occupancy are bonded to C(10) and C(10′), while the minor sites with 0.367(4) occupancy are bonded to C(5) and C(5′). Only the major sites are shown in Figure 6. Despite the disorder, however, it is important to realize that the crystallography does confirm the *trans* arrangement of the keto groups within this structure. The major C(10)–O(2) distance (1.267(3) Å) and the minor C(5)–O(1) distance (1.283(5) Å) are indicative of keto groups on the macrocycle periphery.

Crystals of $(py)_2Ni^{II}$(*cis*-$OEPO_2$) were also obtained by diffusion of methanol into a pyridine solution of **7**. These were found to be isomorphous with those of $(py)_2Ni^{II}$(*trans*-$OEPO_2$).

Discussion

Previous work has presumed that the chromatographic fraction characterized as the *trans*-dioxoporphodimethene, **2**, was a pure substance.[2-4] However, as shown here, it consists of two materials, the *trans* compound **2** and its *cis* isomer **5**. Earlier studies had identified another, slower moving red-pink compound for which the structures **8** and **9**, which are related to **5**, were proposed.[2,3]

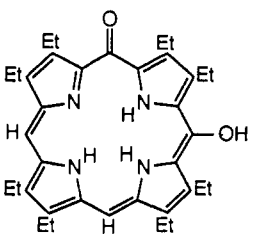

8

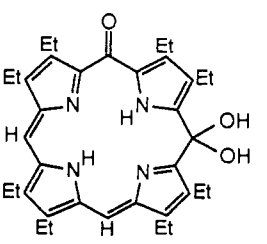

9

More recently another, dimeric structure was proposed for the red-pink material.[4] That substance has not been reinvestigated in the present work, but it is important to note that its spectroscopic properties, which include two, equally intense meso resonances

Table IV. Selected Bond Lengths and Angles for $(py)_2Ni^{II}(trans\text{-}OEPO_2)$[a]

Bond Lengths (Å)			
Ni–N(1)	2.067(2)	Ni–N(2)	2.074(2)
Ni–N(3)	2.223(2)	O(1)–C(5)	1.283(5)
O(2)–C(10)	1.267(3)	N(1)–C(1)	1.371(3)
N(1)–C(4)	1.373(3)	N(2)–C(6)	1.369(3)
N(2)–C(9)	1.365(2)	N(3)–C(19)	1.346(2)
N(3)–C(23)	1.344(3)	C(1)–C(2)	1.436(3)
C(1)–C(10′)	1.442(3)	C(2)–C(3)	1.381(3)
C(5)–C(6)	1.413(2)	C(3)–C(4)	1.439(2)
C(7)–C(8)	1.367(3)	C(4)–C(5)	1.421(3)
C(8)–C(9)	1.449(3)	C(6)–C(7)	1.444(3)
C(9)–C(10)	1.442(3)	C(19)–C(20)	1.365(4)
C(20)–C(21)	1.384(3)	C(21)–C(22)	1.373(3)
C(22)–C(23)	1.381(4)		
Bond Angles (deg)			
N(1)–C(1)–C(2)	111.2(2)	N(1)–C(1)–C(10′)	124.1(2)
N(2)–Ni–N(3)	89.0(1)	N(2)–Ni–N(1′)	89.3(1)
N(3)–Ni–N(1′)	91.0(1)	Ni–N(1)–C(1)	128.3(2)
Ni–N(1)–C(4)	126.0(1)	C(1)–N(1)–C(4)	105.4(2)
Ni–N(2)–C(6)	126.2(1)	Ni–N(2)–C(9)	128.0(2)
C(6)–N(2)–C(9)	105.7(2)	Ni–N(3)–C(19)	122.1(1)
Ni–N(3)–C(23)	121.7(1)	C(19)–N(3)–C(23)	116.2(2)
N(1)–C(1)–C(2)	111.2(2)	N(1)–C(1)–C(10′)	124.1(2)
C(2)–C(1)–C(10′)	124.6(2)	C(1)–C(2)–C(3)	106.2(2)
C(2)–C(3)–C(4)	106.2(2)	C(3)–C(2)–C(11)	126.1(2)
N(1)–C(4)–C(5)	124.6(2)	C(2)–C(3)–C(13)	127.4(2)
O(1)–C(5)–C(4)	116.3(2)	N(1)–C(4)–C(3)	111.0(2)
C(4)–C(5)–C(6)	127.7(2)	C(3)–C(4)–C(5)	124.4(2)
N(2)–C(6)–C(7)	110.7(2)	O(1)–C(5)–C(6)	116.0(3)
C(6)–C(7)–C(8)	106.5(2)	N(2)–C(6)–C(5)	124.6(2)
N(2)–C(9)–C(8)	110.9(2)	C(5)–C(6)–C(7)	124.6(2)
C(8)–C(9)–C(10)	124.6(2)	C(7)–C(8)–C(9)	106.1(2)
O(2)–C(10)–C(1′)	117.5(2)	N(2)–C(9)–C(10)	124.5(2)
C(2)–C(11)–C(12)	113.5(2)	O(2)–C(10)–C(9)	116.8(2)
N(3)–C(19)–C(20)	123.7(2)	C(9)–C(10)–C(1′)	125.7(2)
C(20)–C(21)–C(22)	117.8(2)	C(19)–C(20)–C(21)	119.6(2)
N(3)–C(23)–C(22)	123.4(2)	C(21)–C(22)–C(23)	119.4(2)

[a] Symmetry code: ′ = 1–*x*, 1–*y*, 1–*z*.

at 6.58 and 4.62 ppm in the ^1H NMR spectrum,[2,3] are distinct from those of either *trans*-H_2OEPO_2 (**2**) or the newly identified *cis*-H_2OEPO_2 (**5**).

The solid-state structures of these and related[16,17] OEP derivatives show a remarkably poor ability of the crystalline state to differentiate between closely related molecular geometries. Thus, the tetragonal forms of $Ni^{II}(OEP)$,[14] $Ni^{II}(OEPOH)$,[15] $Ni^{II}(trans\text{-}OEPO_2)$ (**6**), and $Ni^{II}(cis\text{-}OEPO_2)$ (**7**) form an isomorphous set of crystals. This requires disorder in the location of the oxygen atoms for the latter three. As a consequence of this disorder, crystallography is unable to clearly differentiate between the *cis* and *trans* isomers **6** and **7**. Additionally, $(py)_2Ni^{II}(trans\text{-}OEPO_2)$, $(py)_2Ni^{II}(cis\text{-}OEPO_2)$, and $(py)_2Ni^{II}(OEPO^{\bullet})$[15] also form an isomorphous set of crystals. Again there is disorder in the location of the oxygen atoms of $(py)_2Ni^{II}(trans\text{-}OEPO_2)$ and $(py)_2Ni^{II}(OEPO^{\bullet})$. However, there is crystallographic evidence that $(py)_2Ni^{II}(trans\text{-}OEPO_2)$ does indeed have the trans or α,γ orientation of the keto groups. These disorder problems have been noted for several other modified porphyrins in which the modification involves a small perturbation to an internal portion of the macrocycle.[16-19] On the other hand, the external shape of the macrocycle is dictated by its overall size (a flat disk) and the set of external substituents. In the cases described here these substituents are the eight ethyl groups whose locations are clearly similar.

These disorder problems do not, however, plague all structural work on **2** and its metal complexes. The structure of $ClTl^{III}(trans\text{-}OEPO_2)$ is reported to be fully ordered with a slight ruffling of the macrocycle.[20] That study made no mention of a *cis* isomer of the macrocycle.

Both isomers of the dioxo macrocycles have the flexibility to form the saddle-shaped geometry exemplified by $Ni^{II}(cis\text{-}OEPO_2)$ (**7**) and also to assume the flattened shape exemplified by $(py)_2Ni^{II}(trans\text{-}OEPO_2)$. These geometrical changes occur in response to the change in electronic structure of the nickel center. For the diamagnetic, four-coordinate forms with the $d_{x^2-y^2}$ orbital empty, the macrocycle is distorted to accommodate the small size of the nickel(II) ion. However, for the paramagnetic, six-coordinate forms with a single electron in the $d_{x^2-y^2}$ and d_{z^2} orbitals, the Ni–N distances (both in-plane and out-of-plane) are longer and the macrocycle is able to assume a nearly planar geometry. While in the solid state, the saddle-shaped geometry renders each of the protons within a methylene group inequivalent; in chloroform-*d* solution, the ^1H NMR spectra show that the protons of each of the methylene groups of **6** and **7** are equivalent. Since such inequivalencies have been readily resolved in the spectra of other asymmetric H_2OEP derivatives (i.e., $Ni^{II}(OEPN\text{–}O)$),[21] the solution structure must differ from that seen in the solid state. Two explanations are possible. The macrocyclic ligands in **6** and **7** may be planar in solution, or else they are saddle-shaped but are undergoing a rapid inversion from one saddle to another through a planar intermediate or transition state. Cooling a chloroform-*d* solution of $Ni^{II}(trans\text{-}OEPO_2)$ to –60°C produces some minor broadening of the spectrum, but this is not sufficient to allow differentiation between the structural possibilities in solution.

Both $Ni^{II}(cis\text{-}OEPO_2)$ and $Ni^{II}(trans\text{-}OEPO_2)$ display greater axial Lewis acidity than either $Ni^{II}(OEP)$ or $Ni^{II}(OEPOH)$. The latter two dissolve in pyridine, remain diamagnetic, and do not take up added axial ligands.[15] On the other hand, both **6** and **7** readily form paramagnetic, six-coordinate adducts in this solvent. The enhanced axial Lewis acidity is no doubt a consequence of the electronic structure of the macrocycles **2** and **5**. Both of these isomers are more highly oxidized than porphyrins like H_2OEP or H_2OEPOH. This, along with the electron-withdrawing keto substituents on the periphery, probably renders these macrocycles less electron donating and thereby enhances the axial acidity of the nickel centers in **6** and **7**.

Experimental Section

Preparation of Compounds. *trans*-H_2OEPO_2 (2) and *cis*-H_2OEPO_2 (5). A mixture of **2** and **5** was obtained as part of the array of oxidation products that are formed in the reaction of $Zn^{II}(OEP)$ with thallium (III) trifluoroacetate, as previously described.[3] The two isomers were separated from the other products by chromatography on alumina with dichloromethane as eluent.[3] The second, orange-brown fraction was collected and evaporated to yield a (4:1) mixture of **2** and **5**. ^1H NMR (chloroform-*d*) ***trans*-H_2OEPO_2**, δ: 14.64 (2 H, s, NH); 6.67 (2 H, s, meso H); 2.50, 2.71 (16 H, 2 q, methylene H); 1.11, 1.14 (24 H, 2 t, methyl H). ^1H NMR (chloroform-*d*) for ***cis*-H_2OEPO_2**, δ: 14.04, 14.25 (2 H, 2 s, NH); 6.54 (2 H, s, meso H); 2.43–2.79 (m, methylene H); 1.03–1.18 (m, methyl H).

Preparation and Separation of $Ni^{II}(trans\text{-}OEPO_2)$ and $Ni^{II}(cis\text{-}OEPO_2)$. A slurry of a 30.0-mg sample of a mixture of *trans*-H_2OEPO_2 (**1**) and *cis*-H_2OEPO_2 (**5**) in 5 mL of glacial acetic acid was slowly added to a boiling solution of 6.61 mg (0.278 mmol) of nickel(II) acetate tetrahydrate in 25 mL of glacial acetic acid. The green solution became deep orange as metalation proceeded and the macrocycle dissolved. The solid was boiled under reflux for 10 min and then allowed to cool to room temperature. Dichloromethane (50 mL) was added to the solution, which was then washed with five 80-mL portions of water to remove the unreacted nickel acetate and acetic acid. After the dichloromethane

(17) Balch, A. L.; Chan, Y. W.; Olmstead, M. M.; Renner, M. W. *J. Am. Chem. Soc.* **1985**, *107*, 2393.
(18) Latos-Grażyński, L.; Lisowski, J.; Olmstead, M. M.; Balch, A. L. *J. Am. Chem. Soc.* **1987**, *109*, 4428.
(19) Latos-Grażyński, L.; Lisowski, J.; Szterenberg, L.; Olmstead, M. M.; Balch, A. L. *J. Org. Chem.* **1991**, *56*, 4043.
(20) Senge, M. O.; Smith, K. M. *Z. Naturforsch.* **1992**, *47B*, 837.
(21) Balch, A. L.; Chan, Y. W.; Olmstead, M. M. *J. Am. Chem. Soc.* **1985**, *107*, 6510.

layer was dried over sodium sulfate, it was filtered and the filtrate was evaporated to dryness. The dark solid was dissolved in a minimum of benzene and subjected to chromatography on a 30 cm long, 5 cm diameter silica gel column with benzene as the eluent. Generally three bands eluted. The first was a pink band that contained a trace amount of Ni^{II}(OEP) that arose from any unreacted H_2OEP that was carried along from the initial thallium oxidation. The second ochre band was collected and evaporated to dryness to yield 20.6 mg (69%) of Ni^{II}(*trans*-$OPEO_2$). Further elution produced a closely spaced violet band, which was collected and evaporated to dryness to give 5.5 mg (18%) of Ni^{II}(*cis*-$OPEO_2$). The complexes could be recrystallized by dissolution in chloroform and precipitation through the addition of methanol.

Ni^{II}(*trans*-$OEPO_2$). ^{1}H NMR ($CDCl_3$, 22 °C), δ: 6.08 (2 H, s, meso); 2.12, 2.20 (16 H, 2 q, methylene); 0.92, 0.95 (24 H, 2 t, methyl). UV/vis, λ_{max}, nm (ϵ, M^{-1} cm^{-1}): in CH_2Cl_2, 337 (46 000), 458 (138 000), 546 (26 000), 676 (6000); in pyridine, 332 (28 000), 447 (80 000), 542 (sh) (11 000), 584 (14 000), 780 (sh) (360), 850 (450). IR (mineral oil mull), ν(C=O) 1627 sh, 1600.

Ni^{II}(*cis*-$OEPO_2$). ^{1}H NMR ($CDCl_3$, 22 °C), δ: 5.84 (2 H, s, meso); 2.04, 2.12, 2.20, 2.30 (16 H, 4 q, methylene H); 0.87, 0.91, 0.98, 1.00 (24 H, 4 t, methyl). UV/vis, λ_{max}, nm (ϵ, M^{-1} cm^{-1}): in CH_2Cl_2, 323 (9000), 386 (13 000), 548 (5000), 998 (1000); in pyridine, 310 (7000), 337 (9000), 371 (12 000), 386 (13 000), 433 (7000), 545 (4000), 897 (1000), 991 (1000). IR (mineral oil mull), cm^{-1}: ν(C=O) 1732, 1589.

X-ray Data Collection. Ni^{II}(*cis*-$OEPO_2$) (7). Black prisms were obtained by slow diffusion of methanol into a chloroform/trifluoroacetic acid (99:1 v/v) solution of the complex. The crystals were coated with a light hydrocarbon oil, and a selected crystal was placed in the 130 K dinitrogen stream of a Siemens P4/Ra diffractometer that was equipped with a low-temperature apparatus. Two check reflections showed only random (<2%) fluctuations in intensity during data collection. The data were corrected for Lorentz and polarization effects. Crystal data are given in Table V.

Ni^{II}(*trans*-$OEPO_2$) (6). Very small, dark, flattened octahedra were obtained by diffusion of methanol into a chloroform/trifluoroacetic acid (99:1 v/v) solution of the complex. A crystal of dimensions 0.02 × 0.03 × 0.04 mm was examined. It formed in the tetragonal space group $I4_1/a$ with a = 14.637(7) Å and c = 14.091(7) Å, and thus it is isomorphous with the *cis* isomer **7**.

$(py)_2Ni^{II}$(*trans*-$OEPO_2$). Dark orange parallelepipeds were obtained by slow diffusion of methanol into a pyridine solution of Ni^{II}(*trans*-$OPEO_2$). The crystal was mounted as described above. Crystal data are given in Table V. IR (mineral oil mull), cm^{-1}: ν(C=O) 1624, 1582.

$(py)_2Ni^{II}$(*cis*-$OEPO_2$). Dark crystals were obtained by diffusion of methanol into a pyridine solution of the complex. These formed in the triclinic space group $P\bar{1}$ with a = 9.8551(19) Å, b = 10.2110(17) Å, c = 10.4909(14) Å, α = 80.176(12)°, β = 89.606(13)°, and γ = 66.582(13)° at 130 K. Since they were isomorphous with $(py)_2Ni^{II}$(*trans*-$OPEO_2$), further work on them was not pursued. IR (mineral oil mull), cm^{-1}: ν(C=O) 1731, 1590.

Solution and Refinement of Structures. Ni^{II}(*cis*-$OEPO_2$). Calculations were performed on a Micro VAX 3200 computing system with the Siemens SHELXTL PLUS software package. The structure was solved by direct methods. Anisotropic thermal parameters were assigned to the nickel, oxygen, nitrogen, and carbon atoms. Hydrogen atoms were refined at calculated positions through the use of a riding model in which the C–H vector was fixed at 0.96 Å. Scattering factors and corrections for anomalous dispersion were taken from a standard source.[22] The final stages of refinement included an absorption correction with a method that obtains an empirical absorption tensor from an expression that relates F_o and F_c.[23] The largest peak in the final difference map had a value of 0.23 e Å^{-3}.

Table V. Crystal Structure Data

	Ni^{II}(*cis*-$OEPO_2$)	$(py)_2Ni$(*trans*-$OEPO_2$)
formula	$C_{36}H_{42}N_4NiO_2$	$C_{46}H_{50}N_6NiO_2$
fw	621.4	777.6
space group	$I4_1/a$, tetragonal	$P\bar{1}$, triclinic
a, Å	14.664(7)	9.878(4)
b, Å		10.212(4)
c, Å	14.163(7)	10.503(4)
α, deg		80.08(3)
β, deg		89.28(3)
γ, deg		66.50(3)
V, Å^3	3045(3)	955.2(6)
Z	4	1
T, K	130	130
λ(Cu Kα), Å	1.541 78	1.541 78
μ, mm^{-1}	1.225	1.107
d_{calc}, Mg/m^3	1.355	1.352
transm factors	0.83–0.88	0.90–0.94
no. of reflns	745	2149
no. of params	102	260
R^a	0.039	0.030
R_w^b	0.043	0.040

^{a} $R = \sum||F_o| - |F_c||/\sum|F_o|$. ^{b} $R_w = \sum||F_o| - |F_c||w^{1/2}/\sum|F_o|w^{1/2}$.

$(py)_2Ni^{II}$(*trans*-$OEPO_2$). The solution and refinement followed the procedure outlined above. There was disorder in the position of the oxygen atoms. The refined occupancy of O(1) was 0.367(4), and that of O(2) was 0.633(4). The largest peak in the final difference map had a value of 0.18 e Å^{-3}.

Instrumentation. ^{1}H NMR spectra were recorded on a General Electric QE 300 Fourier transform spectrometer. Magnetic moments were measured in solution by the Evans technique.[24] Electronic spectra were obtained through the use of a Hitachi U-2000 spectrophotometer.

Acknowledgment. We thank the NIH (Grant GM26226) for financial support.

Supplementary Material Available: Tables of bond distances, bond angles, anisotropic thermal parameters, hydrogen atom coordinates, and crystal structure refinement data for Ni^{II}(*cis*-$OPEO_2$) and $(py)_2Ni^{II}$(*trans*-$OPEO_2$) (11 pages). Ordering information is given on any current masthead page.

(22) *International Tables for X-ray Crystallography*; D. Reidel Publishing Co.: Boston, MA, 1992; Vol. C.
(23) Moezzi, B. Ph.D. Thesis, University of California, Davis, CA, 1987.
(24) Evans, D. F. *J. Chem. Soc.* **1959**, 2003.